RESEARCH ARTICLE

# Identification and Distribution Characteristics of Mudstone Intercalations in Ultra-Deep Tight Fractured Sandstone Gas Reservoirs: A Case Study of the Keshen A Gas Reservoir, Tarim Basin

**Yanan Li**[1,2], **Changan Shan**[1,2,*] **and Xinwu Mi**[3]

[1] School of Earth Sciences and Engineering, Xi'an Shiyou University, Xi'an 710065, China
[2] Shaanxi Key Lab of Petroleum Accumulation Geology, Xi'an Shiyou University, Xi'an 710065, China
[3] Korla Branch of GRI of BGP Inc., Korla 841000, China

## Abstract

**The ultra-deep tight sandstone gas reservoirs in the Tarim Basin, exemplified by the Keshen A gas reservoir, face escalating challenges of water invasion and pressure maintenance after years of production. Interlayers within these reservoirs serve as critical geological barriers, yet their spatial distribution remains poorly resolved due to limitations in conventional identification methods. This study integrates core, logging, 3D seismic, and production data within a sequence stratigraphic and reservoir geology framework to establish a "core-logging-seismic" collaborative identification system for argillaceous interlayers. Two main interlayer types—argillaceous and physical—are identified within the Bashijiqike Formation. Argillaceous interlayers exhibit distinctive logging responses ("high GR, high AC, low resistivity"), and seismic half-width attributes effectively delineate their lateral distribution. These interlayers are predominantly concentrated in the K1bs2 interval, with thicknesses of 0.8–2.5 m and a NW-SE oriented planar distribution. Based on thickness and lateral extent, they are classified into three levels (single-well, well-group, and reservoir-scale). Interlayers exceeding 1.5 m in thickness with good lateral continuity form effective flow barriers that significantly suppress water invasion. The findings were applied to well-pattern optimization in 2023, reducing overall water influx by 37% and increasing estimated recovery by 8.2%, supporting a transition from empirical to geologically-guided development in ultra-deep tight reservoirs.**

**Keywords**: keshen block, cretaceous, tight sandstone, mud interlayer, multi-scale recognition, water intrusion prevention and control.

**Submitted:** 29 December 2025
**Accepted:** 20 January 2026
**Published:** 02 February 2026

**Vol.** 2, **No.** 1, 2026.
10.62762/JGEE.2025.797111

***Corresponding author:**
✉ Changan Shan
shanca@xsyu.edu.cn

**Citation**
Li, Y., Shan, C., & Mi, X. (2026). Identification and Distribution Characteristics of Mudstone Intercalations in Ultra-Deep Tight Fractured Sandstone Gas Reservoirs: A Case Study of the Keshen A Gas Reservoir, Tarim Basin. *Journal of Geo-Energy and Environment*, 2(1), 34–45.

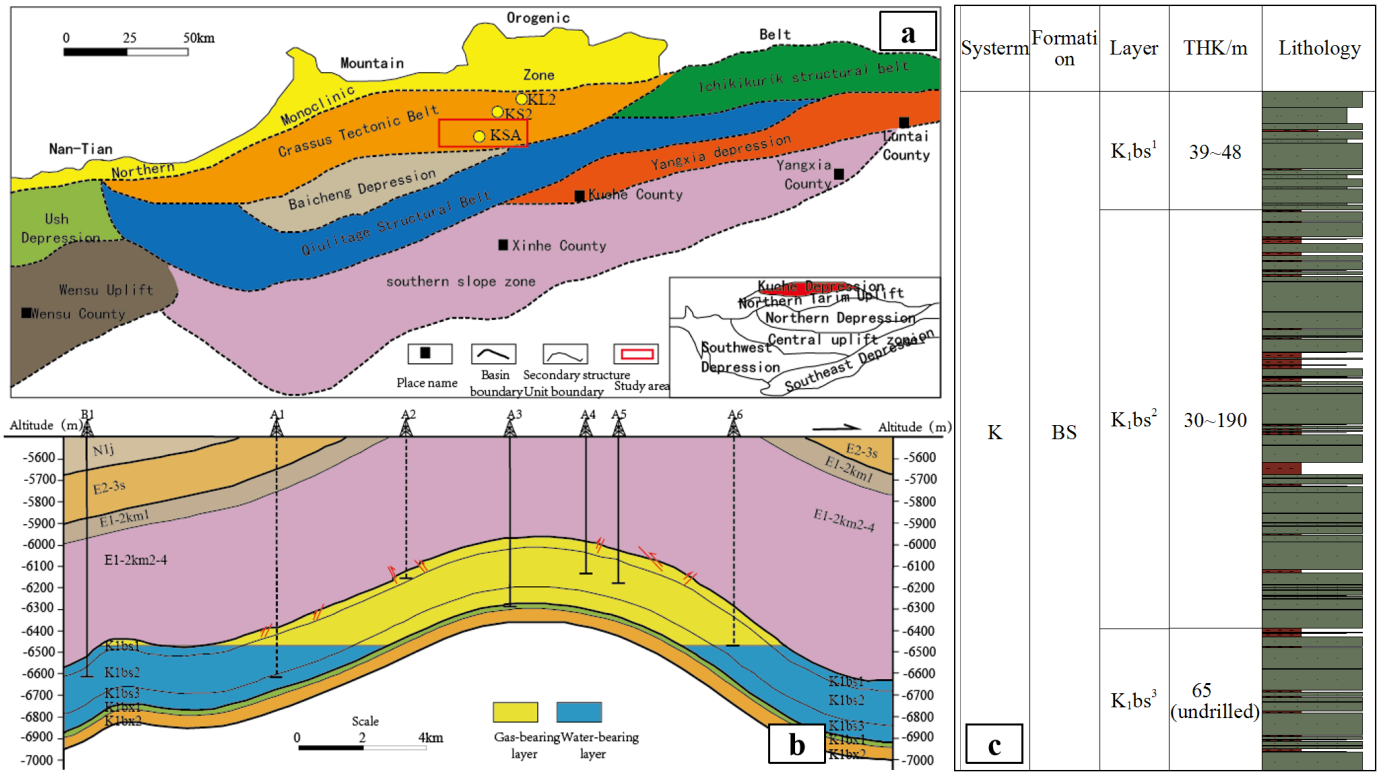


**Figure 1.** The regional location (a), east-west gas reservoir profile (b) and stratigraphic histogram (c) of Keshen A gas reservoir in Kuqa Depression, Tarim Basin.

## 1 Introduction

The Tarim Basin is the largest superimposed composite oil and gas basin in China.Its northern Kuqa Depression develops extremely thick high-quality source rocks with high hydrocarbon generation intensity, and the abundance of oil and gas resources ranks among the top in China [1, 2]. The buried depth of Keshen gas reservoir is generally more than 6500 m, and the proven reserves are more than $5000 \times 10^8$ $m^3$. It is the main gas source of the West-East Gas Pipeline Project, which is of great strategic significance to ensure national energy security and regional economic development [3]. However, the geological conditions in this area are complex, the tectonic activity is strong, the reservoir is buried deep, the heterogeneity is strong, and the stress is high, resulting in high exploration and development costs. In recent years, with the advancement of the development process, water has been found in many production wells. The water cut of some wells has risen rapidly, and the pressure of stable production has been increasing. Water invasion has become a core problem restricting the efficient development of gas reservoirs [4].

The predecessors have carried out a lot of research on the key geological factors such as fracture system, fracture network, stress field distribution and reservoir heterogeneity of Keshen gas reservoir, and achieved fruitful results [5–7]. However, the research on interlayers in tight sandstone reservoirs is still relatively weak. The traditional geophysical methods have insufficient recognition accuracy for thin interlayers with a thickness of less than 5m, resulting in unclear spatial distribution of interlayers and difficulty in effectively guiding development and adjustment. Especially in ultra-deep tight sandstone gas reservoirs, interlayer is not only an important manifestation of reservoir heterogeneity, but also a key geological barrier to control fluid migration and delay water invasion. Its identification and characterization need to be broken through.

In this paper, Keshen A gas reservoir is taken as the research object, and a multi-scale collaborative identification method of "core-logging-seismic" is innovatively constructed. Through fine core description, logging response calibration, seismic attribute optimization and waveform inversion, the development types, identification marks and spatial distribution characteristics of argillaceous interlayers are systematically revealed, and the effectiveness of water invasion prevention and control is evaluated in combination with production performance data. The purpose is to provide scientific basis for well pattern optimization, development adjustment and recovery

factor improvement of ultra-deep tight sandstone gas reservoirs.

## 2 Geological Background

The Keshen A gas reservoir is located in the western section of the Kelasu tectonic belt in the Kuqa Depression of the Tarim Basin (Figure 1(a)). It is located in the compressive tectonic system of the leading edge of the South Tianshan orogenic belt. It is controlled by the strong tectonic compression of the Himalayan period. There are many rows of nearly EW-trending thrust faults, forming a typical "faulted anticline" structural style [8]. The main body of the gas reservoir is a north-dipping monoclinic structure, which is cut by secondary reverse faults to form multiple fault block traps. The buried depth of the target layer Bashijiqike Formation is generally more than 6500 m, which belongs to the ultra-deep structural-lithologic composite gas reservoir (Figure 1(b)). The reservoir heterogeneity is strong, the fracture is developed, and the reservoir performance is controlled by both tectonic stress and diagenesis [9].

The sedimentary system of Bashijiqike Formation transits from fan delta (K1bs3) to braided river delta front (K1bs2, K1bs1) from bottom to top, and the vertical differentiation of sedimentary facies is obvious. The K1bs3 section is dominated by fine sandstone and siltstone, with a small amount of thin mudstone, and a set of variegated glutenite at the bottom. The K1bs2 section is brown medium-fine sandstone, with thin to medium-thick brown mudstone and silty mudstone, and local mud gravel enrichment. The K1bs1 section is dominated by brown fine sandstone, with a small amount of siltstone and brown thin mudstone, and local mud gravel [10].

The study area is mainly drilled K1bs1 and K1bs2 sections (Figure 1(c)). The average porosity of the reservoir is 6.8%, and the permeability is 0.15 mD, which is a typical tight sandstone. The diagenesis is strong, mainly quartz overgrowth and carbonate cementation, and the porosity of local structural fracture zone can be increased to more than 9% [11].

The interlayer is mainly developed in the reservoir, which is mainly composed of argillaceous interlayer (32%), calcareous cementation layer (57% ) and tight sandstone physical interlayer (11%). The thickness of the interlayer is 0.3-3.0 m, and the lateral continuity is poor, but the multi-stage sealing system is formed in the vertical direction, which controls the vertical differentiation of the gas reservoir and the distribution of the pressure system [12]. Among them, the argillaceous interlayer is mostly developed in the sedimentary environment of underwater interdistributary bay, and the lithology is reddish brown mudstone or silty mudstone, which is in sudden contact with the upper and lower sand layers. The physical interlayers are mostly distributed in areas with strong diagenesis. The lithology is argillaceous siltstone or siltstone, with dense cementation and poor pore connectivity. There are significant differences in physical properties, sedimentary environment and genetic mechanism between the two types of interlayers, which are the key geological factors controlling fluid migration [13].

## 3 Sequence Stratigraphic Framework

A systematic understanding of the Cretaceous sequence stratigraphic framework in Kuqa Depression has been formed. Combined with core, logging and seismic data, the Cretaceous can be divided into one first-order sequence (tectonic sequence), three second-order sequences (sedimentary cycle) and eight third-order sequences. The first-order sequence corresponds to the regional tectonic subsidence event caused by the strong thrust of the South Tianshan Mountains, covering the whole Cretaceous period. The second-order sequence is controlled by the tectonic-climate cycle, showing the sedimentary response of progradation-retrogradation alternation. The third-order sequence is related to short-term sea level fluctuation and provenance activity [14].

The Bashijiqike Formation constitutes a complete third-order sequence as a whole. The upper interface corresponds to the regional parallel unconformity surface at the bottom of the Paleogene Kumugeliemu Group, and the lower boundary is the sedimentary structure transition surface at the top of the Brazilian cover group. The sequence can be further divided into lowstand system tract (Ba3 member), transgressive system tract (K1bs2) and highstand system tract ( K1bs1 ), and the maximum flooding surface is located at the boundary between K1bs1 and K1bs2 [15].

In order to finely identify the sequence interface, this paper uses INPEFA (Integrated Prediction Error Filter Analysis) curve analysis method to enhance the ability of sedimentary cycle identification by filtering the natural gamma curve. Taking Well A3 as an example, combined with core and logging data, the K1bs1 and K1bs2 sections are divided into 8 sub-sections : K1bs1-1, K1bs1-2 (2 sub-sections) ; k1bs2-1 to K1bs2-6

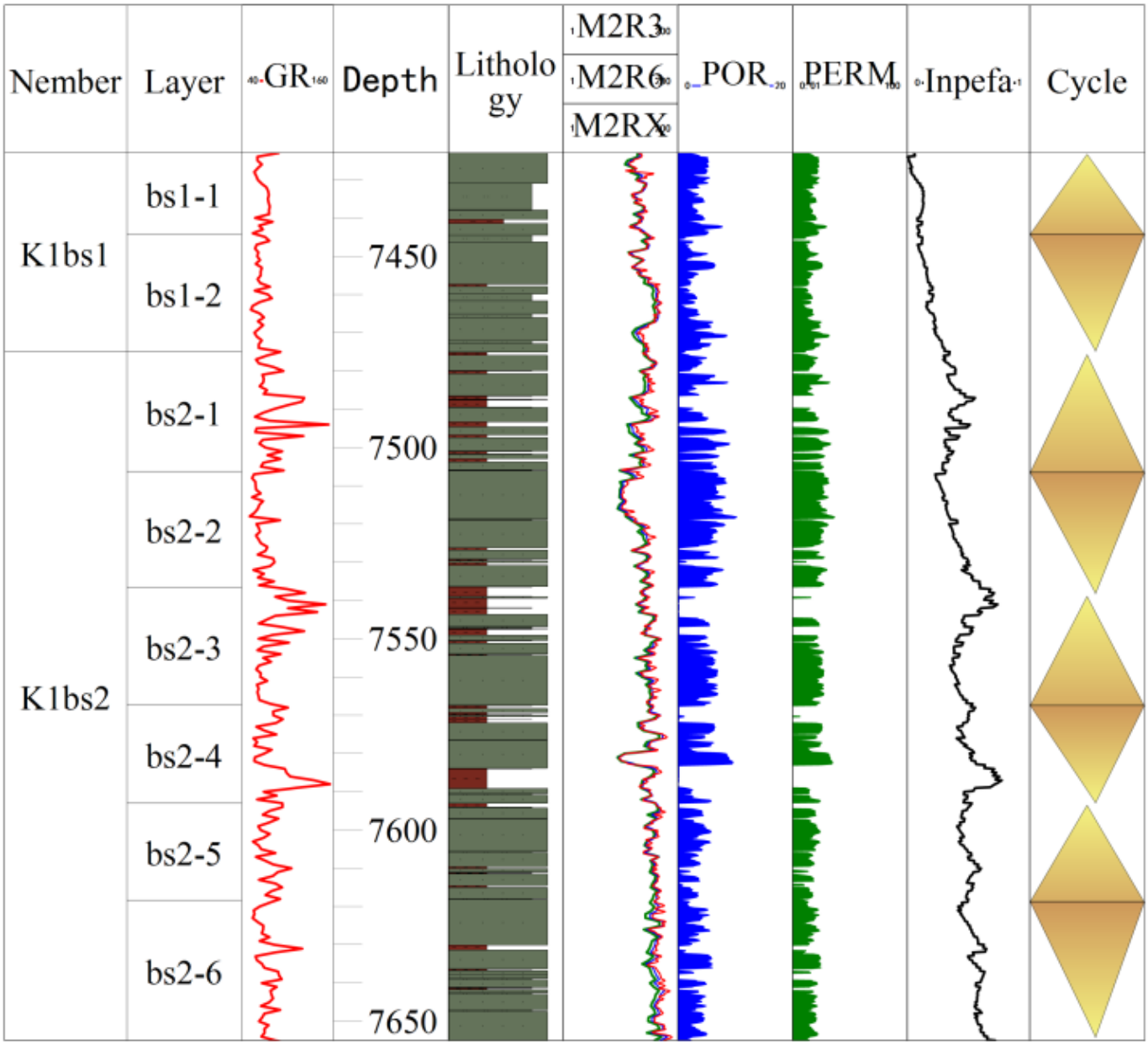


**Figure 2.** Stratigraphic map of Well A3 in Keshen A gas reservoir divided by INPEFA method.

(6 sub-segments) (Figure 2).

The comparison of wells shows that the thickness distribution of each sub-section is stable, with an average thickness of 20-35 m. Most wells in the area are drilled to the K1bs2-3 sub-section (Figure 3). The results of sequence division provide a reliable geological framework for the subsequent identification and distribution of interlayers [16].

## 4 Interlayer identification method and technical route

Aiming at the problem of low accuracy and strong multi-solution of thin interlayer identification in ultra-deep tight sandstone reservoirs, this paper constructs a three-step identification method of " core calibration-logging quantification-seismic constraint " to realize multi-scale collaborative identification from micro to macro and from point to surface.

### 4.1 Core identification: the bridge between microstructure and macroscopic lithology

Core observation is the basis of interlayer identification. Based on the core system description of two coring wells (A3 and A6) in Keshen A gas reservoir, combined with the analysis of casting thin sections, this paper clarifies that there are two types of interlayers in the

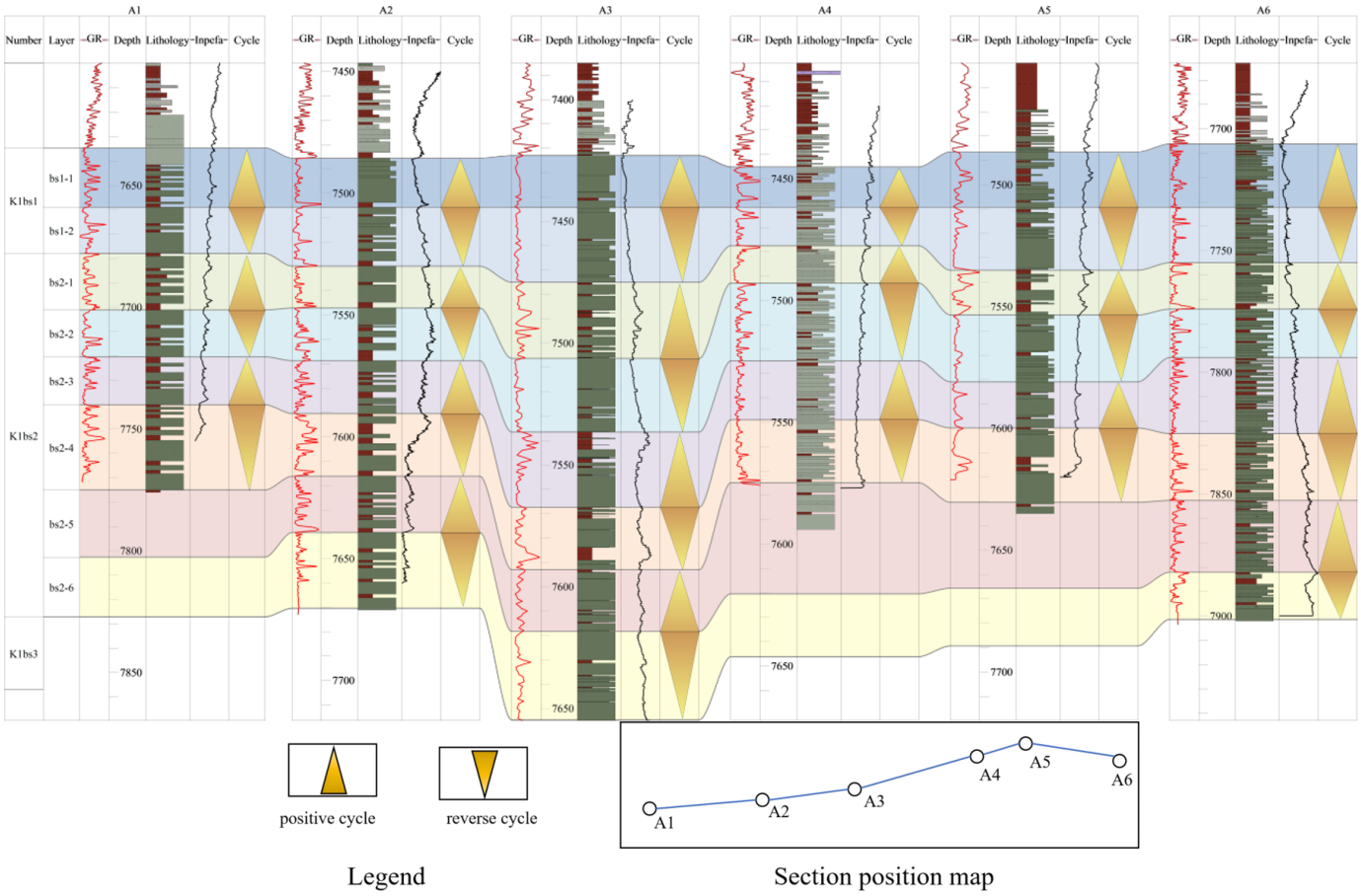


**Figure 3.** Kashen A gas reservoir Bashijiqike formation stratigraphic division correlation well diagram.

reservoir, namely argillaceous and physical properties.

Muddy interlayer: The lithology is mainly reddish-brown mudstone and silty mudstone (Figure 4(a)). The thickness of single layer is 0.3-1.5m, which is in sudden contact with the upper and lower sand layers. The thin sections under the microscope show that the debris is mainly fine sand (particle size 0.05-0.25 mm), containing about 15% argillaceous patches. The interstitial material is mainly argillaceous, coated with thin film particles and filled with intergranular, containing a small amount of dolomite, anhydrite and other cements. The rock debris composition contains a large amount of mud debris and plastic debris such as siliceous rock and phyllite (20%-35%). Quartz and feldspar generally have secondary enlargement, forming a dense mosaic structure. Several contraction fractures (0.01-0.02 mm in width) (Figure 4(b)) can be seen in the rock, but the porosity is less than 3% and the permeability is less than 0.01 mD, reflecting a weak hydrodynamic sedimentary environment, such as flood overflow or intermittent deposition [17].

Physical property interlayer: the lithology is mainly argillaceous siltstone, the clastic component is mainly fine sand (particle size 0.1-0.25mm), mixed with very fine sand, medium sand and coarse sand (Figure 5(a)), the interstitial material is mainly iron-stained argillaceous and dolomite cement, and the dolomite is uniformly distributed between the grains in an irregular grain shape. Compared with the argillaceous interlayer, the argillaceous content is low, but the secondary enlargement of feldspar is still common. The lithic components are mainly siliceous rock, tuff and intermediate-acid extrusive rock. The rock cementation is dense, only a small amount of intergranular dissolved pores, intragranular dissolved pores and argillaceous micropores are developed, the pore connectivity is poor (Figure 5(b)), the permeability is $< 0.05$mD, the sealing ability is weaker than the argillaceous interlayer, and the vertical direction is mostly local seepage barrier [18].

### 4.2 Logging identification : response characteristics and discriminant criteria

Based on the results of core identification, this paper selects natural gamma (GR), acoustic time difference

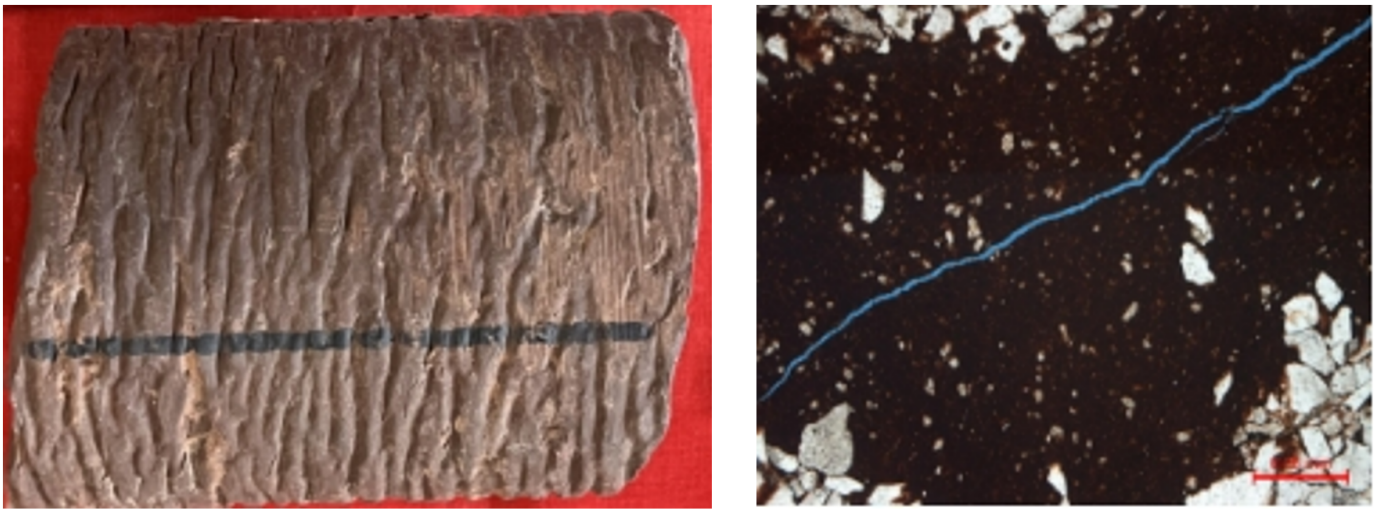

(a) (b)

**Figure 4.** Core photos of muddy interlayer (a) microscopic photos (b).

(a) (b)

**Figure 5.** Core photos of Physical property interlayer (a) microscopic photo (b).

**Table 1.** Standard for logging discrimination of argillaceous interlayers and physical interlayers in Cretaceous Bashijiqike Formation of Keshen A gas reservoir.

| Intercalation Type | GR (API) | AC ($\mu$s/ft) | Density (g/cm$^3$) | Resistivity ($\Omega$·m) | Microelectrode |
|---|---|---|---|---|---|
| Mudstone | 80 (High) | High | Low | Low | Significant return |
| Petrophysical | 80 (Low) | Low | High | High | Minor return |

(AC), resistivity (RT), density (DEN) and neutron (CNL) logging curves to establish the identification criteria of interlayers [19].

**Shale interlayer:** High shale content leads to a significant increase in GR value ($>$ 80API), an increase in AC value ($>$ 200$\mu$s / ft), a decrease in resistivity ($<$ 5$\Omega \cdot$ m), and no significant change in well diameter and density.

**Interlayers with physical properties:** mud content is relatively low, GR value is medium ( $<$ 80API ), AC value is medium and high (180-200$\mu$s/ft), resistivity is medium and high (5-10$\Omega \cdot$ m), well diameter is slightly enlarged, and density is slightly higher (Table 1).

Based on core findings, key logging curves — gamma ray (GR), acoustic transit time (AC), resistivity (RT), density (DEN), and neutron (CNL) — were used to establish discrimination criteria (Table 1).

**Mudstone Intercalations:** High clay content results

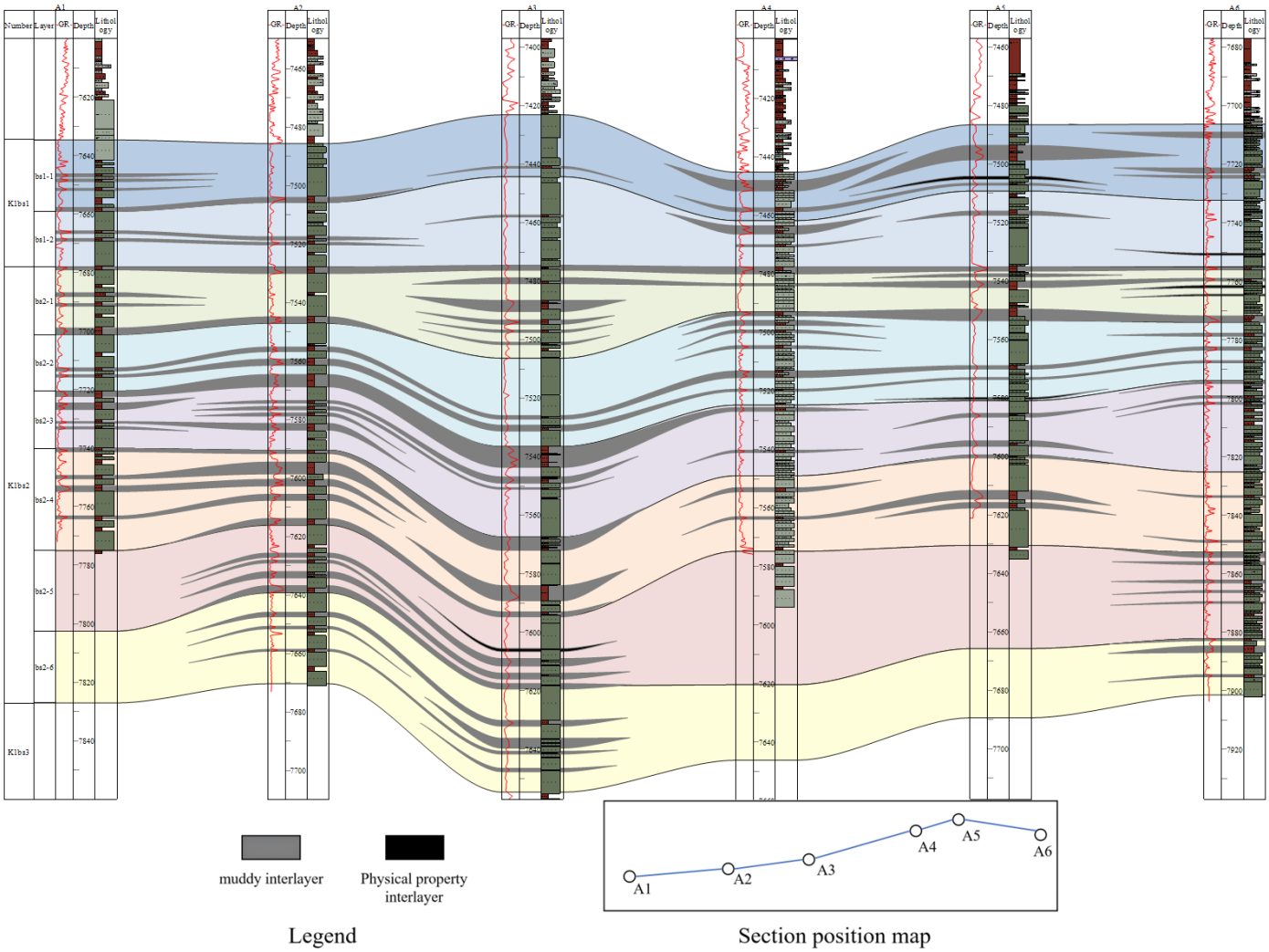


**Figure 6.** Interlayer connecting well profile of Bashijiqike Formation in Keshen A gas reservoir.

in elevated GR (>80 API), increased AC (>200 $\mu$s/ft), reduced resistivity (<5 Ω·m), and borehole enlargement. Density shows minimal variation, yielding a "one high, two lows" signature.

**Petrophysical Intercalations:** Lower clay content leads to moderate GR (<80 API), moderate AC (180–200 $\mu$s/ft), moderate resistivity (5–10 Ω·m), slight borehole enlargement, and slightly higher density.

Through the analysis of single well logging curves, two layers of argillaceous interlayers were identified in the K1bs2-4 sub-section of Well A1, with thicknesses of 1.2 m and 0.8 m, respectively. A layer of physical interlayer was identified in the K1bs1-2 sub-section, with a thickness of 0.6 m. The comparison of wells shows that the argillaceous interlayer is mainly developed in the K1bs2 section, and the physical interlayer is mostly distributed in the K1bs1 section (Figure 6).

### 4.3 Seismic identification: macroscopic distribution and attribute optimization

Although the vertical resolution of seismic data is limited (generally 10-20m), its high-density spatial sampling ability can effectively reflect the lateral variation of formation lithology and fluid information. In ultra-deep tight sandstone gas reservoirs, the thickness of interlayers is mostly less than 5 m, which is difficult to be effectively identified by conventional seismic inversion methods. To this end, this paper introduces a more mature seismic waveform inversion technology, combined with logging constraints and seismic attribute guidance, to achieve high-precision spatial characterization of thin-layer interlayers [20].

### 4.4 Basic principle of seismic waveform indication inversion

Seismic waveform inversion is a multi-scale collaborative inversion method, which is constrained by seismic waveform, corrected by logging data and

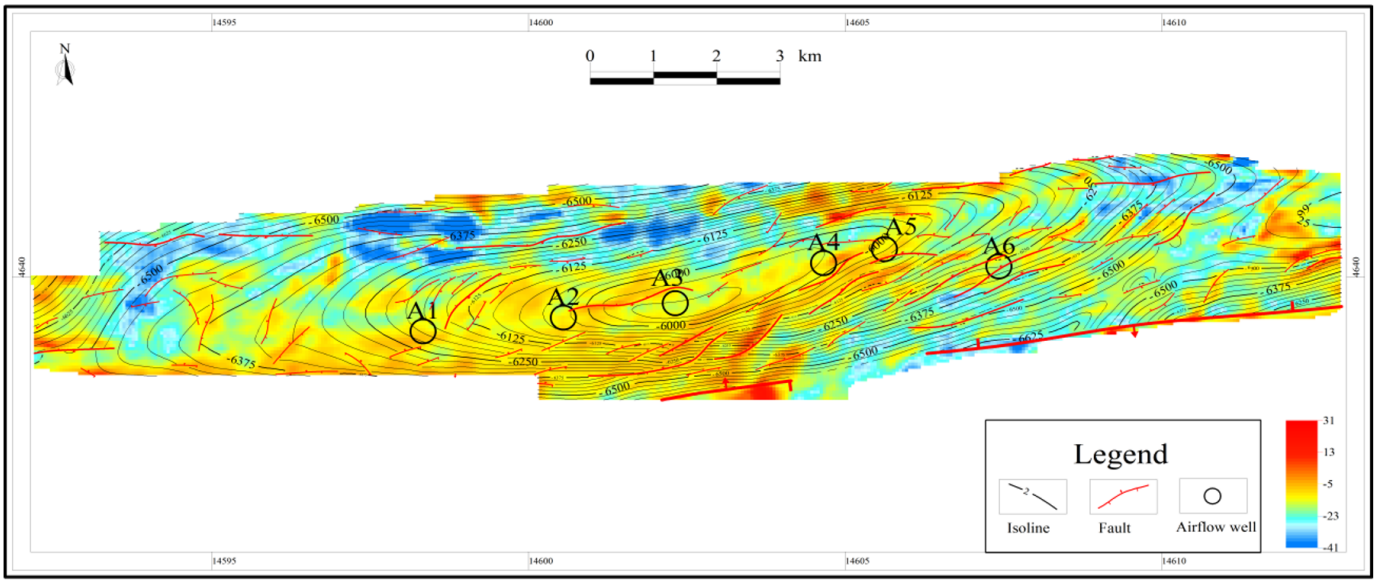


**Figure 7.** Seismic wave half-broadband attribute plane diagram.

guided by geological model. The core idea is that the morphological changes of seismic waveforms are closely related to the underground lithologic interface and physical property mutations. Through waveform similarity matching, the spatial distribution of formation physical parameters can be inverted [21].

This method breaks through the limitation that traditional post-stack inversion only relies on amplitude information, and introduces waveform morphological features (such as peak-valley position, waveform width, phase change, etc.) as inversion constraints, which significantly improves the recognition ability of thin layers and heterogeneous bodies [22].

#### 4.4.1 *Technical process of waveform indication inversion in interlayer identification*

In this paper, the four-step process of "attribute guidance-waveform matching-logging constraint-iterative optimization" is used to realize the fine description of the spatial distribution of interlayers:

Attribute guidelines: The wave half-width attribute is used as the key parameter for interlayer identification. This attribute reflects the width between inflection points of reflection waveform and is sensitive to lateral lithological changes. The half-width of the wave plane shows that the interlayer between K1bs1 and K1bs2 is concentrated in the middle of the study area, and the whole is distributed in the north-south-west direction (Figure 7).

Waveform matching: seismic traces are extracted from the target horizon and matched with the synthetic seismic traces near the well. Through the dynamic time warping algorithm, the similarity coefficient between each seismic waveform and the well-side waveform is calculated, and the ' waveform similarity body ' is constructed as the initial constraint of inversion [23, 24].

Logging constraints: The parameters such as shale content, porosity, and permeability calibrated by the core are converted into wave impedance or elastic parameters as hard constraints for inversion. Through the joint correction of well and seismic, it is ensured that the inversion results are consistent with the logging data at the well point [25].

Iterative optimization: The seismic phase-controlled nonlinear stochastic inversion method is used to gradually optimize the model parameters, so that the synthetic seismic response and the actual seismic data can achieve the best matching in waveform shape and amplitude [26].

#### 4.4.2 *Inversion results and verification*

The inversion results show that the muddy interlayer between K1bs1 and K1bs2 is continuously distributed in the NW-SE direction, with a thickness of 1.0-2.7 m and good lateral continuity (Figure 8). Compared with the actual drilling data of 4 verification wells, the recognition coincidence rate is 82%, and the inversion thickness error is less than 15%.

Further in-depth analysis shows that in the interlayer development section, the seismic waveform shows significant amplitude attenuation, frequency reduction

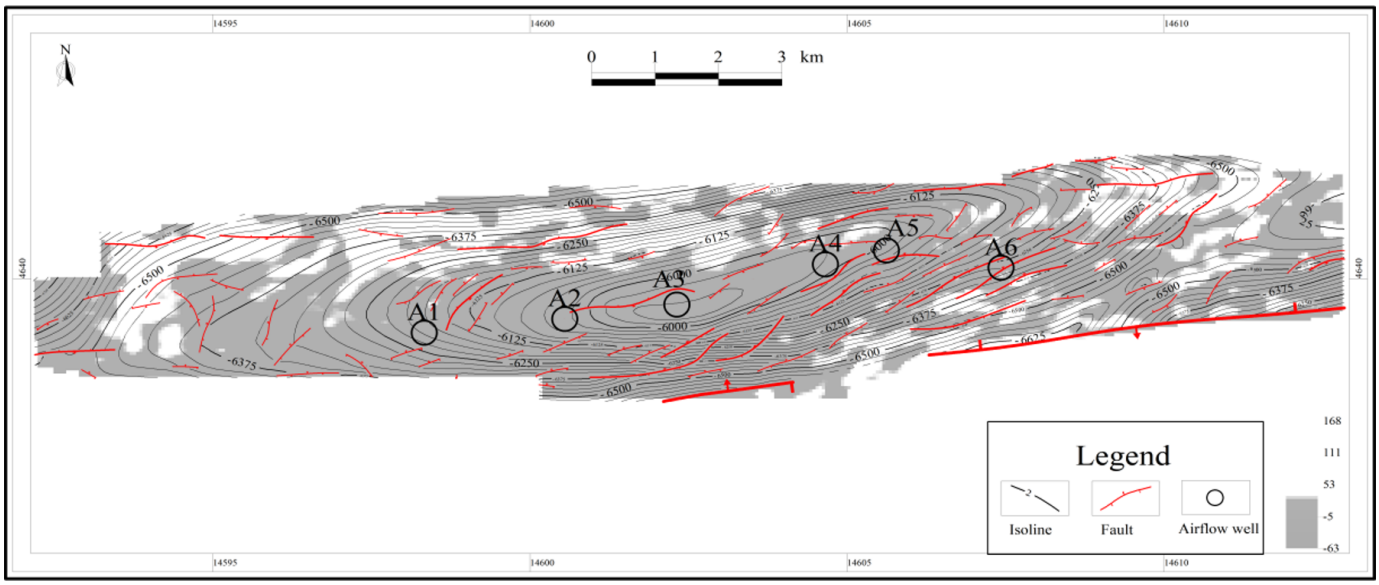


**Figure 8.** Seismic inversion interlayer thickness plane diagram.

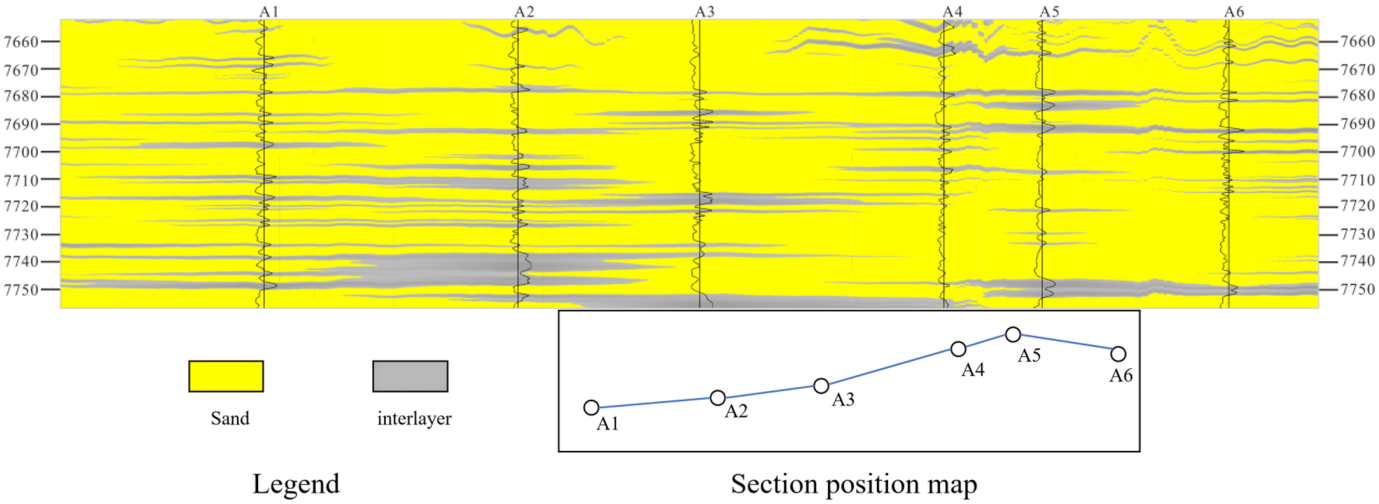


**Figure 9.** Seismic inversion interlayer well comparison profile.

and wave half-width increase, which are in sharp contrast to the non-development section. Through the observation of the waveform similarity body, it can be found that the shape of the waveform has a significant mutation at the boundary of the interlayer (Figure 9). This phenomenon has a high degree of consistency and matching with the interlayers identified in logging data, which further verifies the unique performance of interlayers in seismic response.

### *4.4.3 Technical advantages and applicability*

Compared to conventional post-stack inversion methods, seismic waveform inversion offers several distinct advantages:

**Enhanced thin-layer identification capability:** By incorporating waveform shape constraints, this method can identify interlayers with thicknesses less than 5 meters, thereby overcoming the resolution limitations inherent in traditional inversion techniques.

**Reduced solution non-uniqueness:** Waveform matching constraints effectively suppress the inherent non-uniqueness of inversion results, leading to improved reliability in subsequent geological interpretation.

**Improved characterization of lateral continuity:** The derived waveform similarity volume effectively reflects lateral variations in lithology, assisting in the delineation of interlayer distribution boundaries.

**Compatibility with multi-type data:** The method facilitates the integration of multi-source information, including well-logging data, core samples, and various seismic attributes, enabling multi-scale collaborative inversion.

This approach is particularly well-suited for the characterization of complex, heterogeneous reservoirs with thin-layer development, such as ultra-deep tight sandstone gas reservoirs, shale gas reservoirs, and fractured-vuggy carbonate reservoirs. It finds practical application in critical engineering tasks such as water invasion prevention and control, as well as well pattern optimization.

## 5 Interlayer distribution characteristics and effectiveness evaluation

### 5.1 Vertical distribution characteristics

The interlayers are developed in each small layer of Bashijiqike Formation in Keshen A gas reservoir, but the thickness is thin, mainly 0.8-2.7 m. Among them, the development density of mudstone interlayer in K1bs2 section is high, and K1bs1 section is relatively undeveloped. A set of regional mudstone interlayers developed between K1bs1 and K1bs2, with a thickness of 1.5-2.5 m and good lateral continuity, which is the key geological barrier to control the vertical differentiation of gas reservoirs.

### 5.2 Plane distribution characteristics

According to the comparison between seismic inversion and well logging, the argillaceous interlayer is distributed in NW-SE direction in the plane, which is concentrated in the middle of the study area. The thickness contour shows that the maximum thickness area is located between Well A1 and Well A2, with a thickness of 2.5 m, and gradually thins to 0.8 m on the east and west sides. The physical property interlayers are scattered, mostly patchy, with poor lateral continuity, mainly distributed in the high parts of the structure.

### 5.3 Interlayer classification and effectiveness evaluation

Based on thickness and lateral extension characteristics, interlayers are classified into three distinct levels:

**Single-well level:** Characterized by thicknesses less than 1.0 meter and poor lateral continuity, these interlayers exert only localized effects on individual well production performance.

**Well-group level:** With thicknesses ranging from 1.0 to 1.5 meters and lateral extensions exceeding 500 meters, interlayers at this level can form localized seepage barriers that influence fluid flow within well groups.

**Gas-reservoir level:** Featuring thicknesses greater than 1.5 meters, good lateral continuity, and extensions exceeding 1000 meters, these interlayers form effective barriers against water invasion at the reservoir scale, significantly impacting overall recovery efficiency.

Production dynamic data demonstrate that interlayers at the well-group level and above significantly delay water invasion. The A1 well group, deployed within an interlayer-developed area, exhibits a slow water-cut increase after production, with a water invasion rate 37% lower than adjacent well groups. In contrast, the A3 well group without interlayer protection experiences rapid water content increase, reaching 15% within three months of production commencement.

## 6 Conclusions and suggestions

The three-step identification method of “core calibration-logging quantification-seismic constraint ” is innovatively constructed to effectively reduce the multi-solution of ultra-deep thin interlayer identification and improve the identification accuracy.

The reservoir of Bashijiqike Formation in Keshen A gas reservoir is widely developed with two types of shale and physical interlayers. The shale interlayer has the characteristics of “high GR, high AC and low resistivity”, and the response of the physical interlayer is relatively weak.

The facies-controlled waveform inversion technology can realize the fine prediction of the spatial distribution of muddy interlayers, which are mainly developed in the K1bs2 section, with a thickness of 0.8-2.5m and a NW-SE banded distribution on the plane; the regional mudstone interlayer between K1bs1 and K1bs2 is the key geological barrier to control water invasion.

The interlayer above the well group level can significantly delay the water invasion, and the research results have guided the well pattern adjustment in 2023, which reduces the water invasion rate of the gas reservoir by 37%, and is expected to increase the recovery rate by 8.2%.

It is suggested that the quantitative evaluation of the genetic mechanism and plugging capacity of the interlayer should be further carried out in the follow-up study, and the well pattern deployment should be optimized in combination with numerical simulation to promote the transformation of ultra-deep tight sandstone gas reservoirs from “ empirical development ” to “ geosteering development ”.

## Data Availability Statement

Data will be made available on request.

## Funding

This work was supported without any funding.

## Conflicts of Interest

Xinwu Mi is affiliated with the Korla Branch of GRI of BGP Inc., Korla 841000, China. The authors declare that this affiliation had no influence on the study design, data collection, analysis, interpretation, or the decision to publish, and that no other competing interests exist.

## AI Use Statement

The authors declare that no generative AI was used in the preparation of this manuscript.

## Ethical Approval and Consent to Participate

Not applicable.

## References

[1] HE, D. L., & WU, X. (2013). Comparison in petroleum geology between Kuqa depression and Southwest depression in Tarim Basin and its exploration significance. *Acta Petrolei Sinica, 34*(2), 201. [CrossRef]

[2] Qun, L. E. I., Yun, X. U., Zhanwei, Y. A. N. G., Bo, C. A. I., Xin, W. A. N. G., Lang, Z. H. O. U., ... & Liwei, W. A. N. G. (2021). Progress and development directions of stimulation techniques for ultra-deep oil and gas reservoirs. *Petroleum Exploration and Development, 48*(1), 221-231. [CrossRef]

[3] Jiang, T., & Sun, X. (2019). Development of Keshen ultra-deep and ultra-high pressure gas reservoirs in the Kuqa foreland basin, Tarim Basin: Understanding and technical countermeasures. *Natural Gas Industry B, 6*(1), 16-24. [CrossRef]

[4] Wang, R., Zhang, C., Chen, D., Yang, F., Li, H., & Li, M. (2022). Microscopic Seepage Mechanism of Gas and Water in Ultra-Deep Fractured Sandstone Gas Reservoirs of Low Porosity: A Case Study of Keshen Gas Field in Kuqa Depression of Tarim Basin, China. *Frontiers in Earth Science, 10*, 893701. [CrossRef]

[5] Xusheng, G. U. O., Xiaoxiao, M. A., Maowen, L. I., Menhui, Q. I. A. N., & Zongquan, H. U. (2023). Mechanisms for lacustrine shale oil enrichment in Chinese sedimentary basins. *Oil & Gas Geology, 44*(6), 1333-1349. [CrossRef]

[6] Chonglong, G. A. O., Jian, W. A. N. G., Jun, J. I. N., Ming, L. I. U., Ying, R. E. N., Ke, L. I. U., ... & Yi, D. E. N. G. (2023). Heterogeneity and differential hydrocarbon accumulation model of deep reservoirs in foreland thrust belts: A case study of deep Cretaceous Qingshuihe Formation clastic reservoirs in southern Junggar Basin, NW China. *Petroleum Exploration and Development, 50*(2), 360-372. [CrossRef]

[7] Zhai, M., Wang, D., Zhang, Z., Zhang, L., Yang, F., Huang, B., ... & Li, L. (2022). Numerical simulation and multi-factor optimization of hydraulic fracturing in deep naturally fractured sandstones based on response surface method. *Engineering Fracture Mechanics, 259*, 108110. [CrossRef]

[8] Wang, K., Zhang, R., Zeng, Q., & Wang, J. (2022). Formation mechanism and hydrocarbon exploration significance of the box fold in the Qiulitage structural belt, the Kuqa Depression, Tarim Basin, China. *Journal of Natural Gas Geoscience, 7*(6), 333-346. [CrossRef]

[9] Song, X., Lü, X., Shen, Y., & Guo, S. (2019). Hydrocarbon migration and accumulation history in deep reservoirs: A case study of Mesozoic sandstone gas reservoirs in the Kelasu-Yiqikelike structural belt of the Kuqa Depression, Tarim Basin. *Geosciences Journal, 23*(1), 69-86. [CrossRef]

[10] Zhiyong, G. A. O., Yongping, W. U., Zhaolong, L. I. U., Cong, W. E. I., Cuili, W. A. N. G., & Qunming, L. I. U. (2023). Development model and significance of favorable lithofacies association of sandy braided river facies of the Cretaceous Bashijiqike Formation in Zhongqiu 1 well block, Kuqa Depression, Tarim Basin. *Oil & Gas Geology, 44*(5), 1141-1158. [CrossRef]

[11] Wang, R., Gang, W., Huang, Z., Guo, X., Pan, Y., Zhao, L., & Mo, T. (2025). The Sources of Diagenetic Fluids and Diagenetic Evolution Model in Deep-to-Ultra-Deep Tight Sandstone Reservoirs: A Case Study From Bashijiqike Formation, Kalesu Belt, Kuqa Depression, Tarim Basin, NW, China. *Geological Journal*. [CrossRef]

[12] Deng, J., Liu, M., Ji, Y., Tang, D., Zeng, Q., Song, L., ... & Lian, C. (2022). Controlling factors of tight sandstone gas accumulation and enrichment in the slope zone of foreland basins: The Upper Triassic Xujiahe Formation in Western Sichuan Foreland Basin, China. *Journal of Petroleum Science and Engineering, 214*, 110474. [CrossRef]

[13] Chen, D., Zhang, C., Yang, M., Li, H., Wang, C., Diwu, P., ... & Wang, Y. (2024). Research on water invasion law and control measures for ultradeep, fractured, and low-porosity sandstone gas reservoirs: A case study of Kelasu gas reservoirs in Tarim Basin. *Processes, 12*(2), 310. [CrossRef]

[14] Mingxiang, M., Bingsong, Y., & Weiguang, J. (2004). Sequence Stratigraphy of the desert system: A case study of the Lower Cretaceous in the Kuqa Basin in Xinjiang, northwestern China. *Acta Geologica Sinica-English Edition, 78*(3), 744-755. [CrossRef]

[15] Wen, C., & Wang, Z. (2024). Quantitative Evaluation

and Evolution of Overpressure in the Deep Layers of a Foreland Basin: Examples from the Lower Cretaceous Bashijiqike Formation in the Keshen Area, Kuqa Depression, Tarim Basin, China. *Sustainability, 16*(24), 10884. [CrossRef]

[16] Li, J., Wei, C., Ma, X., & Yu, H. (2015, October). Application of sequence stratigraphy framework in improving the precision of seismic inversion. In *SEG International Exposition and Annual Meeting* (pp. SEG-2015). SEG.

[17] Yang, W., Liu, M., Wei, G., Jin, H., Xie, W., Wu, S., ... & Wang, X. (2021). Lithofacies paleogeography and characteristics of large-scale reservoirs of the Middle Triassic Leikoupo Formation in Sichuan Basin, China. *Journal of Natural Gas Geoscience, 6*(5), 255-268. [CrossRef]

[18] Tingting, K. A. N. G., Fengquan, Z. H. A. O., Lu, F. A. N. G., Haonan, T. I. A. N., Guo, Y. A. N. G., Fangjie, H. U., ... & Liangang, Y. A. N. G. (2022). Sequence stratigraphy and sedimentary facies of pebbled sandstones in coastal system and their controlling effect on the development of high quality reservoirs: Case study of Tazhong 2 well block, Tarim Basin. *Natural Gas Geoscience, 33*(5), 731-741. [CrossRef]

[19] Li, Q., Ren, D., Wang, H., Sun, H., Li, T., Zhang, H., ... & Qu, L. (2024). Microscopic characteristics of tight sandstone reservoirs and their effects on the imbibition efficiency of fracturing fluids: A case study of the Linxing area, Ordos Basin. *Energy Geoscience, 5*(3), 100302. [CrossRef]

[20] Qi, Y., Wu, K., Li, Q., Zheng, X., Wang, B., Li, D., & Tang, W. (2025). Seismic prediction technology for thin reservoirs of tight gas in coal measure strata: a case study of Block L in the eastern margin of the Ordos Basin. *Frontiers in Earth Science, 12*, 1487487. [CrossRef]

[21] Chatterjee, S., Zhao, H., & Zhang, S. (2025, November). Seismic Waveform-Driven Characterization Using Full Frequency Inversion (FFI): A Case Study in Enhanced Seismic Reservoir Characterization from the North-West Shelf, Offshore Australia. In *Abu Dhabi International Petroleum Exhibition and Conference* (p. D041S158R001). SPE. [CrossRef]

[22] Yongshou, Z., Peiling, M., Ning, Y., Xiaochuan, Y., Yaozu, H., & Wei, L. (2024, October). Application of seismic inversion constrained geological modeling technology in quantitative characterization of thin reservoirs. In *Journal of Physics: Conference Series* (Vol. 2834, No. 1, p. 012206). IOP Publishing. [CrossRef]

[23] Li, X., Chen, Q., Wu, C., Liu, H., & Fang, Y. (2016). Application of multi-seismic attributes analysis in the study of distributary channels. *Marine and Petroleum Geology, 75*, 192-202. [CrossRef]

[24] Niu, C., Wang, J. H., Ye, Y. F., Ling, Y., Wang, C., Wang, D., & Zhou, P. (2024). Depth-domain well–seismic calibration method and application based on constrained dynamic warping. *Applied Geophysics*, 1-16. [CrossRef]

[25] Lideng, G., Xiaofeng, D. A. I., Linggao, L. I., Wenhui, D. U., Xiaohong, L. I. U., Yinbo, G. A. O., ... & Shufang, M. A. (2012). Key technologies for seismic reservoir characterization of high water-cut oilfields. *Petroleum exploration and development, 39*(3), 391-404. [CrossRef]

[26] Xie, Q., Wu, Y., Huang, Q., Hu, Y., Hu, X., Guo, X., ... & Wu, B. (2023). Prediction of Marine Thin Shale Gas Reservoir with Seismic Phase-Controlled Nonlinear Stochastic Inversion. *Processes, 11*(8), 2301. [CrossRef]

**Yanan Li** received the B.S. degree in Material Forming and Control Engineering from Dalian University, Dalian 116000, China, in 2015. (Email: 1306639457@qq.com)

**Changan Shan** received the Ph.D. degree in Mineral Resource Prospecting and Exploration from Southwest Petroleum University, Chengdu 610500, China, in 2016. (Email: shanca@xsyu.edu.cn)

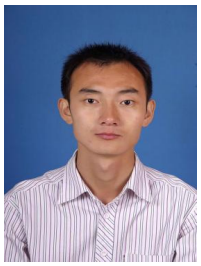

**Xinwu Mi** received the B.S. degree in Resource Exploration Engineering from Southwest Petroleum University, Chengdu 610500, China, in 2009. (Email: mixinwu@cnpc.com.cn)